Military Technical College
Kobry El-Kobbah,
Cairo, Egypt

10th International Conference
on Electrical Engineering
ICEENG 2016

Application of a Global Minimization Technique for Depth Profile Inversion

By

E. A. M. El Fayome [*]
A. H. Kamel [‡]
H. S. ElHennawy [#]

Abstract:

Three simulated annealing cooling schedules (exponential, fast and Boltzmann) are designed, implemented and compared for performance on a depth profile inversion problem. The analysis of the performance results proves that the simulated annealing technique is able to solve nontrivial inverse problems.

Keywords:

Global minimization, simulated annealing

* Ministry of Interior
‡ Advanced Industrial, Technical and Engineering Center
\# Electronics and Communications Department, Faculty of Engineering, Ain Shams University

1. Introduction:

The objective of global minimization [1–4] is to find the globally best solution of nonlinear models, in the presence of multiple local optima.

One constructs an objective function which depends on a number of independent variables and proceeds to find the values of those independent variables that lead to the globally smallest error in the objective function. All the global minimization techniques (simulated annealing, genetic algorithm, particle swarm, ant colony, ...) have the ability to escape from a local minimum (in contrast to local minimization methods that are trapped in the first minimum they found).

Simulated annealing is a probabilistic technique for approximating the global optimum of a given function. Specifically, it gives an approximate global optimization in a large search space. For problems where finding the precise global optimum is less important than finding an acceptable global optimum in a fixed amount of time, simulated annealing is preferable to alternative methods.

The technique of simulated annealing [5–6] is based on the physical analogy of cooling crystals that, when cooled very slowly, attempt to arrive at its globally minimal potential energy. The name and inspiration come from annealing in metallurgy, a technique involving heating and controlled cooling of a material to increase the size of its crystals and reduce defects. Both are attributes of the material that depend on its thermodynamic free energy. Heating and cooling the material affects both the temperature and the thermodynamic free energy. While the same amount of cooling brings the same decrease in temperature, the rate of cooling dictates the magnitude of decrease in the thermodynamic free energy, with slower cooling producing a bigger decrease. Simulated annealing interprets slow cooling as a slow decrease in the probability of accepting worse solutions as it explores the solution space. Accepting worse solutions is a fundamental property of the technique because it allows for a more extensive search for the optimal solution through the ability to escape local minima. This is accomplished by simulated annealing acceptance function, namely, if the new objective function value is less than the old, the new guess is always accepted. Otherwise, the new guess is accepted at random with a probability depending on the difference in objective function values and on the current temperature.

The method was independently described by Scott Kirkpatrick, C. Daniel Gelatt and Mario P. Vecchi in 1983, [7] and by Vlado Černý in 1985, [8]. The method is an adaptation of the Metropolis–Hastings algorithm, a Monte Carlo method to generate sample states of a thermodynamic system, invented by M. N. Rosenbluth and published

by N. Metropolis et al. in 1953.[9]

2. Formulation:

An application of simulated annealing, namely, depth profile inversion is presented. An electric current source of known strength and location in free space emits an electromagnetic field that interacts with an inhomogeneity embedded in free space. The inhomogeneity is in the form of a slab of known thickness and consists of N layers, each of known thickness, with unknown material properties (permittivities and conductivities).

The electromagnetic fields scattered from the inhomogeneity are collected at M wave numbers. One would like to find the 2N material properties, given the measured scattered electromagnetic fields at the M wave numbers.

To find the unknowns, one converts the inverse scattering problem into a global minimization one.

An objective function, £, is constructed in the form

$$£ = \sum_{m=1}^{M} |E_m^m - E_c^m|^2, \tag{1}$$

where E_m^m is the measured electric field collected at the m^{th} wave number and E_c^m is the electric field computed from a guess of what the 2N material properties might be. Hence, the objective function is 2N-dimensional, that is,

$$£ = f\left(\{ò_{r,n}\}, \{\sigma_n\},\ n = 1:N\right), \tag{2}$$

where $ò_{r,n}$ and σ_n are the relative permittivity and conductivity, respectively, of the n^{th} layer.

Such a 2N-dimensional function will have many minima. One then looks for the 2N variables that lead to the global minimum of the objective function, which when found will identify the sought after material properties of the layered slab.

3. Design of the algorithm:

A) *Initial Guesses Preparation*

The proposed simulated annealing method is applied on slabs of four layers ($N = 4$). A very large data set of 5^{2N} initial guesses (of where the global minimum might be located

in the 2N-dimensional space) have been generated, with the relative permittivity ($\grave{o}_{r,n}$) and the conductivity (σ_n) with $n = 1:N$, in the form

$$\begin{aligned} \grave{o}_{r,n} &= a_n + b_n \ \mathrm{Rand}(1,1), \\ \sigma_n &= c_n + d_n \ \mathrm{Rand}(1,1), \end{aligned} \tag{3}$$

with Rand(1,1) is a box-car random number generator for values between zero and one. Hence,

$$\begin{aligned} a_n + b_n &\geq \grave{o}_{r,n} \geq a_n, \\ c_n + d_n &\geq \sigma_n \geq c_n. \end{aligned} \tag{4}$$

The ranges in eq. (4) are supposed to be known a priori. We have used in the work presented here

$$\begin{aligned} 2.2 &\geq \grave{o}_{r,1} \geq 1.8, \\ 3.3 &\geq \grave{o}_{r,2} \geq 2.7, \\ 4.4 &\geq \grave{o}_{r,3} \geq 3.6, \\ 5.5 &\geq \grave{o}_{r,4} \geq 4.5, \\ 0.12 &\geq \sigma_1 \geq 0.1, \\ 0.24 &\geq \sigma_2 \geq 0.12 \\ 0.36 &\geq \sigma_3 \geq 0.3, \\ 0.48 &\geq \sigma_4 \geq 0.4. \end{aligned}$$

Next, we select, randomly, from the generated data set, a small percent (typically 0.5%–2%) for using as initial guesses for the simulated annealing algorithm. Figure (1) shows the distribution of one variable, $\grave{o}_{r,4}$, for the initial guess. Since, for the presented case, $5.5 \geq \grave{o}_{r,4} \geq 4.5$, it is to be noted from the figure that the small percent, 1%, retained the box-car distribution of the original very large data set.

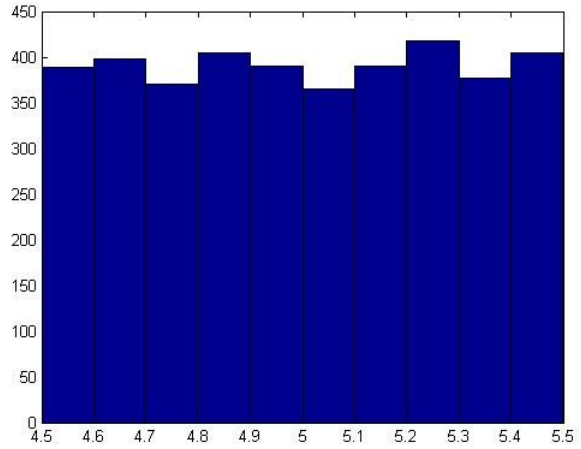

***Figure (1):** Histogram distribution of the initial guess values of the relative permittivity of the fourth layer ($\grave{o}_{r,4}$).*

Hence, the algorithm is not biased to certain initial guess values over other values. Similar figures for the remaining seven variables can be found in [10]. Since, nonetheless, we have a large number of initial guesses –3906– (to test the method) an efficient Maxwell's equation solver is needed to generate the value of the objective function. We have developed and used our own solver, see [10–11] for details.

Three simulated annealing cooling schedules (exponential, fast and Boltzmann) are designed, implemented and compared for performance.

Performance criteria include mean square error (MSE), percent error in each medium parameter for the minimum objective function, error histogram distribution as well as the effect on the results of the test case, of adding different percentages of noise to $\{E_m^m\}$. The test case used for the performance analysis presented here is $\grave{o}_{r,1}=2, \grave{o}_{r,2}=3$, $\grave{o}_{r,3}=4$, $\grave{o}_{r,4}=5$, $\sigma_1=0.11$, $\sigma_2=0.22$, $\sigma_3=0.33$ and $\sigma_4=0.44$. More cases can be found in [10].

B) *Exponential Cooling Schedule (ECS)*

In this case, the cooling schedule is given by

$$T_s = a^s T_0, \tag{5}$$

where $s=1,2,3,\ldots$ is the iteration number (we use 5001 iterations), T_0 is the initial temperature (we used $100\,^{\circ}C$) and a is the cooling rate (we used 0.95).

Table (1) shows the performance of this cooling schedule for noiseless data and ±1% noisy data. Figs. (2)–(3) show the histogram of the distribution of the relative percentage error for $\grave{o}_{r,4}$ (without/with noise). The number of initial guesses used in the work presented here is 3906.

***Table (1):** Performance of ECS*

Noise	0	±1%
Minimum objective function	3.9×10^{-11}	7.39×10^{2}
Percent error in slab parameters	[-0.47, 0.64, 0.73, 2.4, 0.012, 1.1, -0.72, -4.9]	[-9.9, -9.9, 1.9, 9.9, 9.1, -1.8, 9.0, 9.1]
MSE	0.002	0.048

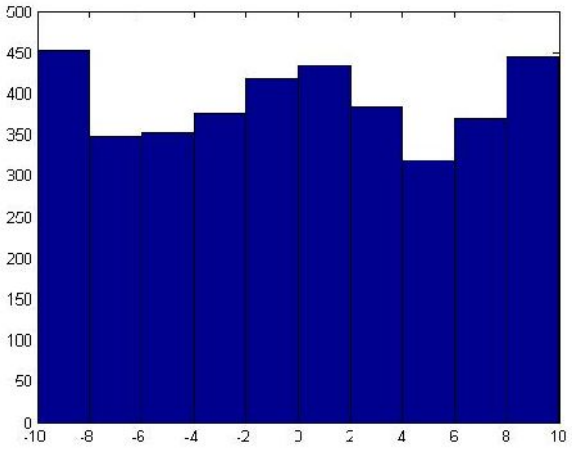

***Figure (2):** Histogram distribution for the percentage error of the relative permittivity of the fourth layer, $\grave{o}_{r.4}$, for the ECS with zero noise.*

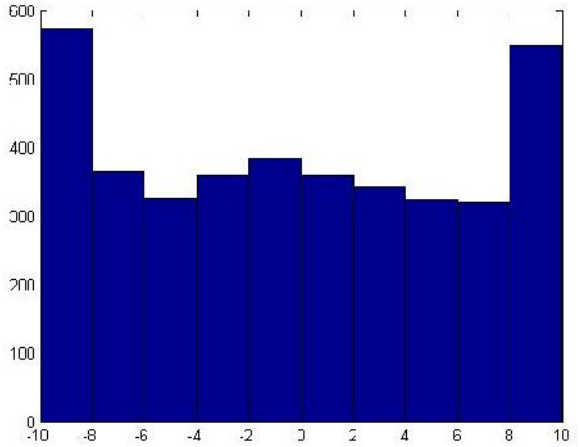

Figure (3): *Histogram distribution for the percentage error of the relative permittivity of the fourth layer, $\grave{o}_{r,4}$, for the ECS with ±1% noise.*

C) *Fast Cooling Schedule (FCS)*

In this case, the cooling schedule is given by

$$T_s = \frac{T_0}{s+1}, \tag{6}$$

where $s = 1, 2, 3, \ldots$ is the iteration number (we use 5001 iterations), T_0 is the initial temperature (we used $100\,^{\circ}C$).

Table (2) shows the performance of this cooling schedule for noiseless data and noisy data. For a fair comparison, the same initial guesses used in B) are used in C). Figs. (4)–(5) show the histogram of the distribution of the relative percentage error for $\grave{o}_{r,4}$ (without/with noise).

Table (2): *Performance of FCS*

Noise	0	±1%
Minimum objective function	6.8×10^{-13}	1.091×10^{3}
Percent error in slab parameters	[-8.8, -1.2, 2.6, -6.4, -0.002, 0.04,-0.19, 0.39]	[-9.45, -10, -3.3, -6, 9.1, 9.1, 9.1, 9.1]
MSE	0.018	0.029

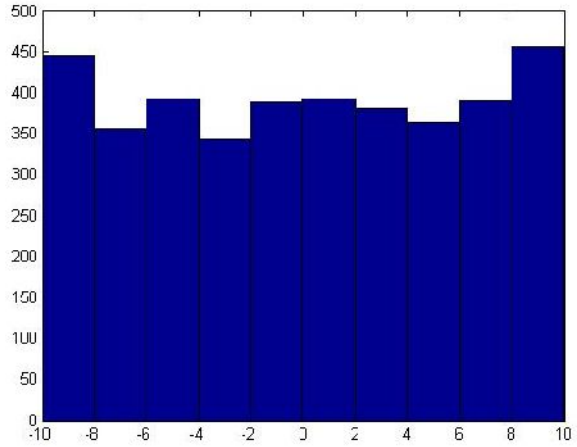

Figure (4): *Histogram distribution for the percentage error of the relative permittivity of the fourth layer, $\grave{o}_{r.4}$, for the FCS with zero noise.*

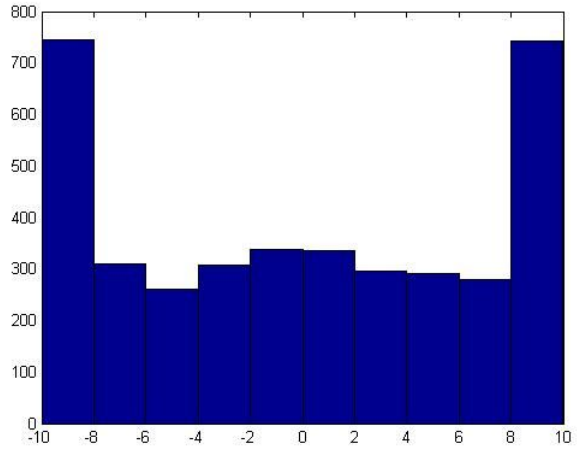

Figure (5): *Histogram distribution for the percentage error of the relative permittivity of the fourth layer, $\grave{o}_{r.4}$, for the FCS with $\pm 1\%$ noise.*

D) *Boltzmann Cooling Schedule (BCS)*

In this case, the cooling schedule is given by

$$T_s = \frac{T_0}{\ln(s+1)}, \tag{7}$$

where $s = 1,2,3,...$ is the iteration number (we use 5001 iterations), T_0 is the initial temperature (we used $100^{\circ}C$).

Table (3) shows the performance of this cooling schedule for noiseless data and $\pm 1\%$

noisy data. For a fair comparison, the same initial guesses used in B) and C) are used in D). Figs. (6)–(7) show the histogram of the distribution of the relative percentage error for $\grave{o}_{r,4}$ (without/with noise).

***Table (3):** Performance of BCS*

Noise	0	±1%
Minimum objective function	2.4×10^{-12}	1.226×10^{3}
Percent error in slab parameters	[-7.5, 1.7, -5.6, 5.0, -0.009, -1.5, 6.6, -1.6]	[9.95, 9.97, -9.99, 10, -9.1, -9.1, -9.1, -9.1]
MSE	0.017	0.068

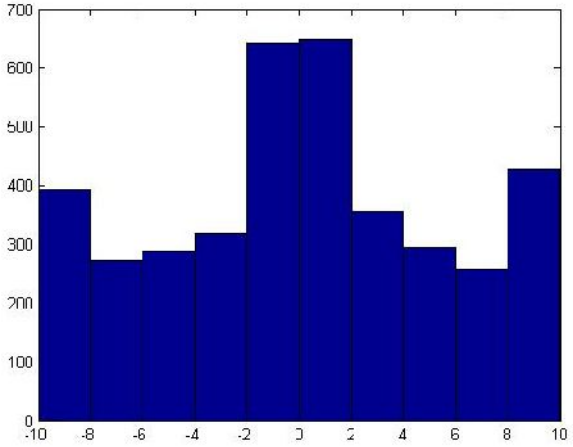

***Figure (6):** Histogram distribution for the percentage error of the relative permittivity of the fourth layer, $\grave{o}_{r,4}$, for the BCS with zero noise.*

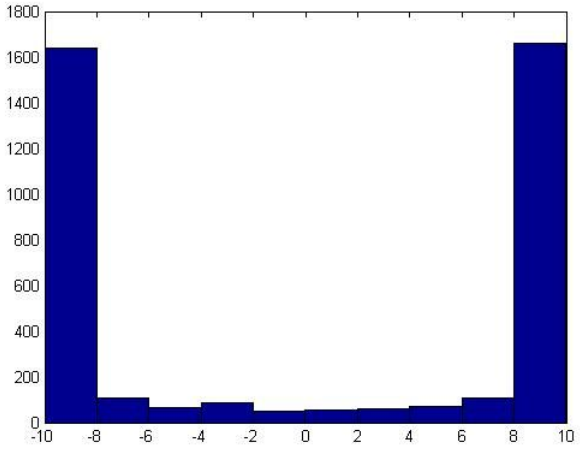

Figure (7): *Histogram distribution for the percentage error of the relative permittivity of the fourth layer,* $\dot{o}_{r,4}$*, for the BCS with* ±1% *noise.*

4. Analysis of the results:

Figure (8) shows the three cooling schedules as functions of s=1:500. The FCS is the fastest while the BCS is the slowest.

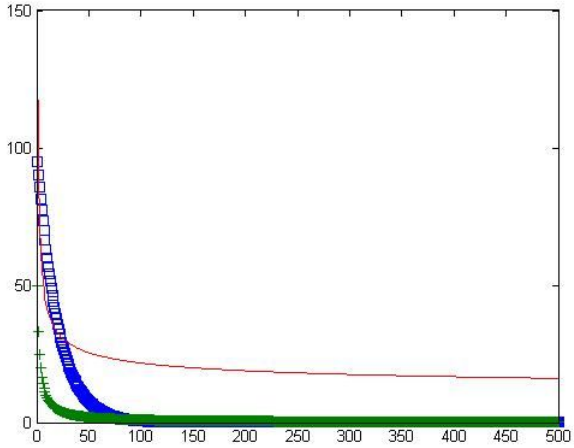

Figure (8): *Cooling schedules. Squares represent the ECS, '+' signs represent the FCS and the solid line represents the BCS.*

The performance results presented here as well as those detailed in [10] show that the ECS has a much better MSE than the FCS and the BCS with the later two of comparable MSE.

The 3906 initial guesses of figure (1). with a priori bound of ±10% led after the

optimization, for the three cooling schedules as per figures (2), (4) and (6) to the same bound of ±10%. Hence, the simulated annealing technique does not improve the a priori knowledge for all the initial guesses taken together.

However, the error in the eight slab parameters for the minimum objective function, as per tables (1)–(3), is much better than the a priori knowledge. The ECS produces the smallest errors with a posteriori major improvement on the a priori knowledge.

Tables (1)-(3) as well as figs. (3), (5) and (7) show that the simulated annealing method is very sensitive to noise; one should not expect an improvement on the a priori known range of each medium parameter. This is in contrast to the artificial neural networks method that continues to produce good results in the presence of noise; see [10].

Figures (2), (4) and (6) also show that the simulated annealing technique does not produce outliers. This is in contrast to the artificial neural networks method that may produce few outliers in the training and/or generalization sets; see [10].

5. Conclusions:

A procedure has been presented and tested for the design of simulated annealing global minimizer for the task of solving inverse scattering problems. While we have concentrated on the role of the cooling schedule, several other parameters should be looked at (for example, the number of iterations). A detailed study of the effect of those parameters can be found in [10]. The analysis of the performance results, for noiseless data, proves that the simulated annealing technique is able to solve nontrivial inverse problems.

References:

[1] E.M.T. Hendrix and B. G.-Tóth, *Introduction to Nonlinear and Global Optimization*. Springer, 2010.
[2] T. Weise, *Global Optimization Algorithms—Theory and Application*, it-weise.de (self-published), 2009.
[3] M. Sen and P. Stoffa, *Global Optimization Methods in Geophysical Inversion*. Elsevier, 1995.
[4] L. Liberti and N. Maculan, *Global Optimization—From Theory to Implementation*, Springer, 2006.
[5] C. M. Tan, *Simulated Annealing*. In-Tech, 2008.
[6] R. Chibante, *Simulated Annealing: Theory with Applications*, Sciyo, 2010.

[7] S. Kirkpatrick, C. D. Gelatt Jr. and M. P. Vecchi, "Optimization by simulated annealing," *Science*, **220** (4598), pp. 671–680, 1983.

[8] V. Černý, "Thermodynamical approach to the traveling salesman problem: An efficient simulation algorithm," *Journal of Optimization Theory and Applications*, **45**, pp. 41–51, 1985.

[9] N. Metropolis, A. W. Rosenbluth, M. N. Rosenbluth, A. H. Teller, and E. Teller, "Equation of state calculations by fast computing machines," *The Journal of Chemical Physics*, **21** (6), pp. 1087–1092, 1953.

[10] E. A. M. ElFayome, *Solutions of Microwave Problems Using VIE*, M.Sc. Thesis, in progress, Electronics and Communications Department, Faculty of Engineering, Ain Shams University, Egypt.

[11] E. A. M. ElFayome, A. H. Kamel, and H. S. ElHennawy, "An alternative formulation for the scattering of electromagnetic waves from vertically stratified media," *ICMA15*, December 27-29, 2015, Egypt.